

Ballistic heat transport of quantum spin excitations as seen in SrCuO₂

N. Hlubek,¹ P. Ribeiro,¹ R. Saint-Martin,² A. Revcolevschi,² G. Roth,³ G. Behr,¹ B. Büchner,¹ and C. Hess¹

¹*IFW-Dresden, Institute for Solid State Research, P.O. Box 270116, D-01171 Dresden, Germany*

²*Laboratoire de Physico-Chimie de L'Etat Solide, ICMMO,*

UMR8182, Université Paris-Sud, 91405 Orsay, France

³*Institut für Kristallographie der RWTH, D-52056 Aachen, Germany*

Fundamental conservation laws predict ballistic, i.e., *dissipationless* transport behaviour in one-dimensional quantum magnets. Experimental evidence, however, for such anomalous transport has been lacking ever since. Here we provide experimental evidence for ballistic heat transport in a $S = 1/2$ Heisenberg chain. In particular, we investigate high purity samples of the chain cuprate SrCuO₂ and observe a huge magnetic heat conductivity κ_{mag} . An extremely large spinon mean free path of more than a micrometer demonstrates that κ_{mag} is only limited by *extrinsic* scattering processes which is a clear signature of ballistic transport in the underlying spin model.

PACS numbers: 75.40.Gb, 66.70.-f, 68.65.-k, 75.10.Pq

The integrability of the one-dimensional (1D) antiferromagnetic $S = 1/2$ Heisenberg chain implies highly anomalous transport properties, in particular, a *divergent* magnetic heat conductivity κ_{mag} at all finite temperatures T .^{1–5} This truly *ballistic* heat transport suggests anomalously large life times and mean free paths of the quantum spin excitations and renders 1D quantum magnets intriguing candidates for spin transport and quantum information processing.^{6–8} However, despite the rigorous prediction, experimental evidence for ballistic heat transport in quantum magnets is lacking. Nevertheless, promising large κ_{mag} has been observed in a number of cuprate compounds which realize 1D $S = 1/2$ Heisenberg antiferromagnets^{9–18} with the spin chain material SrCuO₂ being a prominent example^{10,18} although a quantitative analysis of κ_{mag} has always been difficult there since the phononic and magnetic heat conductivities are of similar magnitude at low temperature. Such experimental κ_{mag} is always *finite* since extrinsic scattering processes due to defects and phonons are inherent to all materials and mask the intrinsic behavior of the chain. Formally it seems reasonable to account for the extrinsic scattering via a finite $\kappa_{\text{mag}} \sim D_{\text{th}}\tau$, where τ is a relaxation time, and D_{th} represents the thermal Drude weight which (multiplied by a delta function at zero frequency) describes the intrinsic heat conductivity. In fact, it was thereby possible to identify the expected low- T linearity of $D_{\text{th}}(T)$ in the case of a “dirty” spin chain material where a high density of chain defects generate a large T -independent scattering rate $1/\tau$.⁹

In this paper we examine the heat conductivity of SrCuO₂ which is considered an excellent realization of the $S = 1/2$ Heisenberg chain.^{19–21} Our samples of extraordinary purity allow an unambiguous separation of the phononic and magnetic contributions to the thermal conductivity. This yields the by far highest κ_{mag} observed^{10,13} until now. Our analysis reveals a remarkable lower bound for the low- T limit of the mean free path l_{mag} of more than a micrometer. Thus our data provide striking evidence that the intrinsic heat transport of the $S=1/2$ Heisenberg chain is indeed ballistic. With

increasing temperatures κ_{mag} is increasingly suppressed due to spinon-phonon scattering which is the dominant extrinsic scattering mechanism in this material.

We have grown large single crystals of SrCuO₂ by the traveling solvent floating zone method,²² where the feed rods were prepared using the primary chemicals CuO and SrCO₃ with both 2N (99%) and 4N (99.99%) purity. Cuboidal samples with typical dimensions of $(3 \times 0.5 \times 0.5)$ mm³ were cut from the crystals, with the longest dimension parallel to the principal axes. Four-probe measurements of the thermal conductivity κ were performed in the 7–300K range²³ with the thermal current along the a , b , and c -axes (κ_a , κ_b , and κ_c respectively) for both the 2N and the 4N samples.

The main structural element in SrCuO₂ is formed by CuO₂ zig-zag ribbons, which run along the crystallographic c -axis (see inset Fig. 1). Each ribbon can be viewed as made of two parallel corner-sharing CuO₂ chains, where the straight Cu-O-Cu bonds of each double-chain structure result in a very large antiferromagnetic intrachain exchange coupling $J/k_B \approx 2100 - 2600$ K of the $S = 1/2$ spins at the Cu²⁺ sites.^{19,21} The frustrated and much weaker interchain coupling $|J'|/J \approx 0.1 - 0.2$ ^{19,24} and presumably quantum fluctuations prevent three-dimensional long range magnetic order of the system at $T > T_N \approx 1.5 - 2$ K $\approx 10^{-3} J/k_B$ K.^{20,25} Hence, at significantly higher T the two chains within one double chain structure can be regarded as magnetically independent. In fact, low- T (12 K) inelastic neutron scattering spectra of the magnetic excitations can be very well described within the $S = 1/2$ Heisenberg antiferromagnetic chain model.²¹

Fig. 1 presents our results for κ_a and κ_c of SrCuO₂ for both 2N and 4N purity as a function of T . We first describe the data for 2N purity which are in good agreement with earlier results by Sologubenko et al.¹⁰ A pronounced low- T peak at ~ 18 K with $\kappa_{\text{max}} \approx 215$ Wm⁻¹K⁻¹ is found for $\kappa_{a,2N}$, i.e., perpendicular to the chains. This peak and a $\sim T^{-1}$ -decrease at $T \gtrsim 150$ K towards a

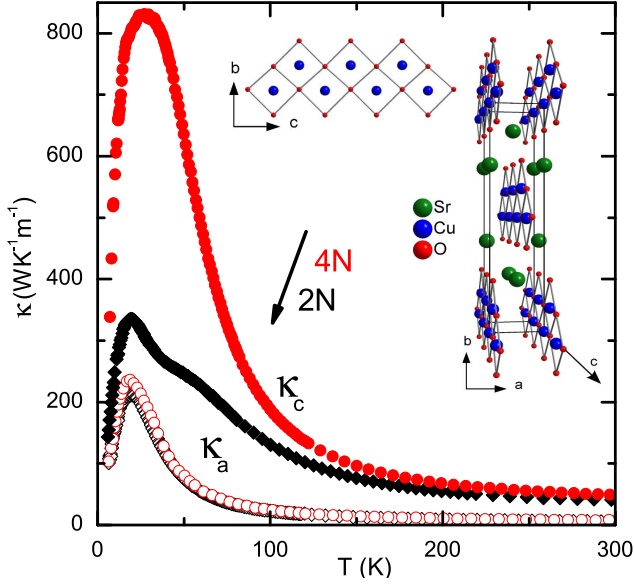


Figure 1: (Color online) κ_a and κ_c of SrCuO_2 for different purity values. Closed (open) symbols represent c -axis (a -axis) data, circles (diamonds) correspond to 4N (2N) purity. Inset: crystal structure of SrCuO_2 . The symmetry is Cmc with lattice constants $a = 3.56$ Å, $b = 16.32$ Å, $c = 3.92$ Å.²⁶

small value at room temperature ($\sim 6 \text{ Wm}^{-1}\text{K}^{-1}$) represent the characteristic T -dependence of phonon-only heat conductivity κ_{ph} . The peak originates from two competing effects:²⁷ at low T , a weakly T -dependent phonon mean free path l_{ph} and a rapidly increasing number of phonons cause κ_{ph} to increase strongly. At higher T , the exponentially rising number of phonon-phonon umklapp processes increasingly shortens l_{ph} , which causes the decrease of κ_{ph} . A similar low- T peak (at ~ 20 K) is also present in $\kappa_{c,2N}$ (parallel to the chains). It is however larger ($\kappa_{\text{max}} \approx 335 \text{ Wm}^{-1}\text{K}^{-1}$) and exhibits a distinct shoulder at the high- T edge ($T \gtrsim 40$ K) of the peak. $\kappa_{c,2N}$ decreases at higher T , but remains much larger than $\kappa_{a,2N}$ and even at room temperature $\kappa_{c,2N} \approx 40 \text{ Wm}^{-1}\text{K}^{-1}$. The apparent large anisotropy, together with the unusual T -dependence of $\kappa_{c,2N}$, is the signature of a large magnetic fraction of $\kappa_{c,2N}$ over a large T -range.^{10,18}

We now turn to the new data which have been obtained for the high-purity compound. The heat transport perpendicular to the chains ($\kappa_{a,4N}$) is slightly enhanced as compared to $\kappa_{a,2N}$ ($\kappa_{\text{max}} \approx 235 \text{ Wm}^{-1}\text{K}^{-1}$) which reflects a somewhat reduced phonon-defect scattering. However, a much more drastic and unexpected large effect of the enhanced purity is observed in the heat transport parallel to the chains, $\kappa_{c,4N}$. Instead of a narrow low- T peak and a shoulder as observed in $\kappa_{c,2N}$, a huge and broad peak centered at ~ 28 K is present in $\kappa_{c,4N}$ ($\kappa_{\text{max}} \approx 830 \text{ Wm}^{-1}\text{K}^{-1}$) which exceeds $\kappa_{c,2N}$ at $T \lesssim 70$ K by more than a factor of 2. Also at $70 \text{ K} \lesssim T \leq 300 \text{ K}$ we observe $\kappa_{c,4N} > \kappa_{c,2N}$, where

interestingly both curves approach each other and at $T \gtrsim 200$ K exhibit almost the same T -dependence.

Without further analysis some clear-cut conclusions can be drawn. First, the extraordinary enhancement of κ_c upon the improvement of the material's purity in contrast to a concomitantly negligibly small one in κ_a , straightforwardly implies that the enhancement primarily concerns the magnetic heat conductivity κ_{mag} which is present in κ_c only. Second, the extreme low- T sensitivity to impurities of κ_{mag} suggests that spinon-defect scattering is the dominating process which relaxes the heat current in this regime. Third, upon rising T , the spinon-defect scattering is increasingly masked by a further scattering process which leads to $\kappa_{c,2N}$ and $\kappa_{c,4N}$ being very similar at $T \gtrsim 200$ K. The most reasonable candidate for this process is spinon-phonon scattering, since the only thinkable alternative, i.e. spinon-spinon scattering, is negligible^{3-5,9} in this T -regime.

A further analysis of the data requires a reliable separation of the total measured κ into all relevant contributions which normally add up. Since electronic contributions can be excluded in this electrically insulating material, it seems natural to assume that the measured κ_c is just the sum of κ_{mag} and a phononic background $\kappa_{\text{ph},c}$,⁹⁻¹⁴ where the latter can be approximated by the purely phononic heat conductivity perpendicular to the chains, $\kappa_a \approx \kappa_b$ (see inset of Fig. 2). The thus obtained $\kappa_{\text{mag}} = \kappa_c - \kappa_a$ for the 2N and the 4N samples are shown in Fig. 2. At $T \lesssim 35$ K, i.e., in the vicinity of the peak of $\kappa_{\text{ph},c}$, errors become large and we disregard the data in this range for further analysis. For higher T we account for a possible uncertainty of $\pm 30\%$ in $\kappa_{\text{ph},c}$. Note that, in the case of the 4N compound, possible errors in κ_{mag} are rendered small because obviously $\kappa_{\text{mag},4N} \gg \kappa_{a,4N}$.

κ_{mag} of the 4N sample exhibits a sharp peak at ~ 37 K with an extraordinary maximum value of about $660 \text{ Wm}^{-1}\text{K}^{-1}$, which is more than a factor of 3 higher than the largest reported κ_{mag} .^{10,13} The peak is followed by a strong decrease upon raising T . Similar to the afore described typical T -dependence of a clean phononic heat conductor, the overall T -dependence of κ_{mag} suggests that, in a simple picture, two competing effects determine κ_{mag} . The low- T increase of κ_{mag} is consistent with a regime where the effect of scattering processes is weakly T -dependent since D_{th} is expected to increase linearly with T .^{3-5,9} The strong decrease at higher T is then the result of the increasing importance of spinon-phonon scattering. κ_{mag} of the 2N sample is qualitatively very similar. However, the absolute value at the peak is much lower ($\sim 172 \text{ W/mK}$) and the peak's position is shifted to a higher T (~ 55 K). Similarly to the κ_c data, at higher T , the 4N curve approaches that of the 2N sample. The latter is consistent with the earlier notion that spinon-phonon scattering is dominant at high T , while the differences at low T suggest that spinon-phonon scattering freezes out, upon decreasing T , rendering spinon-defect scattering increasingly important.

We analyze κ_{mag} quantitatively by extracting the

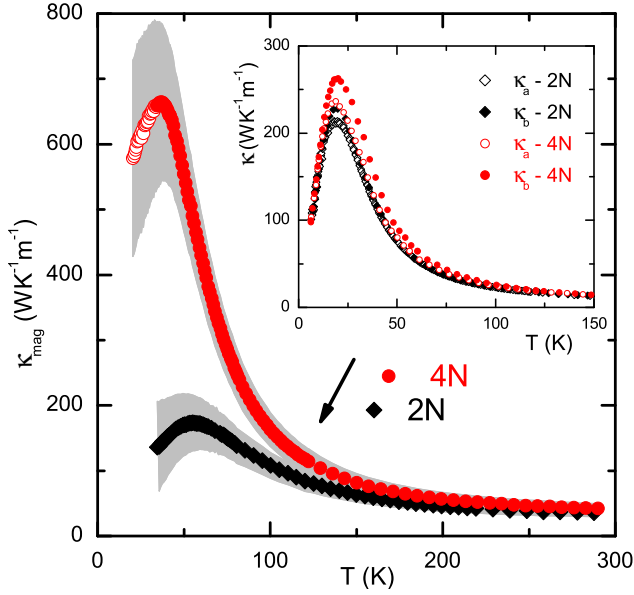


Figure 2: (Color online) κ_{mag} of SrCuO_2 for different purities. Open symbols represent low- T κ_{mag} which is disregarded in the further analysis. The shaded areas show the uncertainty of the estimation of κ_{mag} due to the phononic background. Inset: κ_a and κ_b perpendicular to the chain for both purities.

spinon mean free path l_{mag} according to^{9–11}

$$l_{\text{mag}} = \frac{3\hbar}{\pi N_s k_B^2 T} \kappa_{\text{mag}}, \quad (1)$$

where $N_s = 4/ab$ is the number of spin chains per unit area. As can be inferred from Fig. 3, l_{mag} of both samples show a strong decrease with increasing T , which directly reflects spinon-phonon scattering becoming increasingly important. Both curves are very similar, but clear differences are present at low T , where l_{mag} of the 2N sample is somewhat lower, in accordance with a higher spinon-defect scattering. We evoke Matthiessen's rule to model the T -dependence of l_{mag} and to account for both scattering processes viz. $l_{\text{mag}}^{-1} = l_0^{-1} + l_{\text{sp}}^{-1}$. Here, l_0 describes the T -independent spinon-defect scattering whereas $l_{\text{sp}}(T)$ accounts for the T -dependent spinon-phonon scattering. For the latter, we assume a general umklapp process with a characteristic energy scale $k_B T_u^*$ of the order of the Debye energy, which is commonly used in literature.^{10,15} We thus have

$$l_{\text{mag}}^{-1} = l_0^{-1} + \left(\frac{\exp(T_u^*/T)}{A_s T} \right)^{-1}, \quad (2)$$

which can be used to fit the data with l_0 , A_s and T_u^* (A_s describes the coupling strength) as free parameters. We find an excellent agreement between such fits and the experimental l_{mag} , see Fig. 3. Inspection of the fit parameters³³ yields two remarkable aspects which corroborate our previous qualitative findings. First, the parameters A_s and T_u^* which determine the spinon-phonon

scattering are practically the same for both samples. In fact, an equally good fit is obtained if the *same* T_u^* is used for both curves. Note that the extracted $T_u^* \sim 200$ K is indeed of the order of the Debye temperature Θ_D of this material and thus leads to the conjecture that mostly acoustic phonons are involved in this scattering process.³⁴ Second, the spinon-defect scattering length l_0 , which represents a lower bound for the low- T limit of l_{mag} and which should significantly depend on the sample's purity turns out to be drastically different for both cases. To be specific, we find $l_0 \approx 300$ nm for the 2N compound and an extraordinary $l_0 \approx 1.6$ μm for the 4N sample, which correspond to more than 750 and 4100 lattice spacings, respectively. These findings provide a further confirmation of the above interpretation that, in both cases, κ_{mag} is determined by the same spinon-phonon scattering process and that the difference between the two curves can be described by the different defect density only. We mention that our results are consistent with recent data by T. Kawamata et al.³⁵

A major outcome of our study is the unambiguous identification of the *extrinsic* scattering processes as the only relevant ones. *Intrinsic* spinon-spinon scattering, on the other hand, plays no role in our analysis, even in the case of the very clean sample. The strong enhancement of κ_{mag} upon reduction of the impurity amount thus appears as the manifestation of ballistic heat transport of the underlying spin model, where κ_{mag} is rendered finite by extrinsic scattering processes only. One might therefore speculate that κ_{mag} of this material can be driven to much higher values in a perfect crystal.

We point out that our analysis relies on a very simple theoretical approach which was also successfully used in many other low-dimensional $S = 1/2$ spin systems,^{9–16,28,29} which is surprising in view of the strong quantum nature of such systems. More sophisticated approaches might lead to a deeper understanding of the magnetic heat transport in this system on a microscopic level. In this regard it is interesting to note that, in clean samples (i.e. with large l_0), $l_{\text{sp}} = (A_s T)^{-1} \exp(T_u^*/T)$ leads to $\kappa_c \approx \kappa_{\text{mag}} \propto \exp(T_u^*/T)$ with $T_u^* \sim 200$ K at high T , in agreement with the theory proposed by Shimshoni et al.³⁰ However, we do not observe $\kappa_a = \kappa_{\text{ph}} \propto \exp(2T_u^*/T)$ as expected in the same model. It seems worthwhile mentioning in this regard that the only slight enhancement of κ_a observed upon increasing purity is quite unexpected. One might speculate that this is an indication of phonon scattering off the spin chains which in principle should be relevant.^{31,32}

To sum up, we have investigated the spinon heat conductivity κ_{mag} of the antiferromagnetic $S=1/2$ Heisenberg chain cuprate SrCuO_2 for standard (99%) and high (99.99%) purity. The higher purity leads to a drastic enhancement of κ_{mag} at low T and we find the up-to-present by far highest reported κ_{mag} in the high-purity sample. For higher T , we provide clear-cut evidence that spinon-phonon scattering is the most relevant scattering which leads to a very efficient reduction of κ_{mag} . An extreme

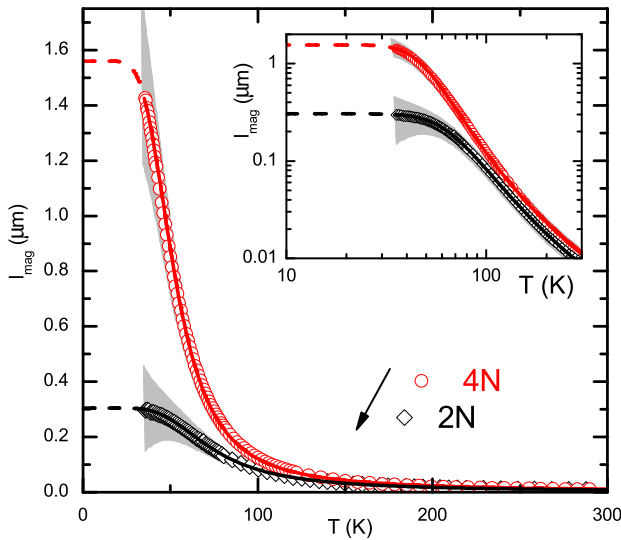


Figure 3: (color online) Magnetic mean free paths of SrCuO_2 for different purities. The solid lines were calculated according to Eq. 2. The shaded area illustrates the uncertainty from the estimation of the phononic background.

sensitivity of κ_{mag} to impurities is present at low T , which implies that the spinon-defect scattering is dominating in this regime. A simple analysis reveals a remarkable lower bound for the low-temperature limit of the spinon mean free path l_{mag} of more than a micrometer. Our results therefore suggest that κ_{mag} is only limited by extrinsic scattering processes which appears as the manifestation of the ballistic nature of heat transport in the $S = 1/2$ antiferromagnetic Heisenberg chain.

Acknowledgments

We thank W. Brenig, A. L. Chernyshev, S.-L. Drechsler, F. Heidrich-Meisner, P. Prelovšek, X. Zotos and A. A. Zvyagin for stimulating discussions. This work was supported by the Deutsche Forschungsgemeinschaft through grant HE3439/7, through the Forschergruppe FOR912 (grant HE3439/8) and by the European Commission through the NOV MAG project (FP6-032980).

- ¹ X. Zotos, F. Naef, and P. Prelovsek, Phys. Rev. B **55**, 11029 (1997).
- ² X. Zotos, Phys. Rev. Lett. **82**, 1764 (1999).
- ³ A. Klümper and K. Sakai, J. Phys. A: Math. Gen. **35**, 2173 (2002).
- ⁴ F. Heidrich-Meisner, A. Honecker, D. C. Cabra, and W. Brenig, Phys. Rev. B **68**, 134436 (2003).
- ⁵ F. Heidrich-Meisner, A. Honecker, and W. Brenig, Phys. Rev. B **71**, 184415 (2005).
- ⁶ F. Meier and D. Loss, Phys. Rev. Lett. **90**, 167204 (2003).
- ⁷ F. Meier, J. Levy, and D. Loss, Phys. Rev. Lett. **90**, 047901 (2003).
- ⁸ L. F. Santos, Phys. Rev. E **78**, 031125 (2008).
- ⁹ C. Hess, H. ElHaes, A. Waske, B. Buechner, C. Sekar, G. Krabbes, F. Heidrich-Meisner, and W. Brenig, PRL **98**, 027201 (2007).
- ¹⁰ A. V. Sologubenko, K. Giannò, H. R. Ott, A. Vietkine, and A. Revcolevschi, Phys. Rev. B **64**, 054412 (2001).
- ¹¹ C. Hess, The European Physical Journal - Special Topics **151**, 73 (2007).
- ¹² A. V. Sologubenko, K. Giannò, H. R. Ott, U. Ammerahl, and A. Revcolevschi, Phys. Rev. Lett. **84**, 2714 (2000).
- ¹³ C. Hess, C. Baumann, U. Ammerahl, B. Büchner, F. Heidrich-Meisner, W. Brenig, and A. Revcolevschi, Phys. Rev. B **64**, 184305 (2001).
- ¹⁴ C. Hess, H. ElHaes, B. Büchner, U. Ammerahl, M. Hücker, and A. Revcolevschi, Phys. Rev. Lett. **93**, 027005 (2004).
- ¹⁵ T. Kawamata, N. Takahashi, T. Adachi, T. Noji, K. Kudo, N. Kobayashi, and Y. Koike, Journal of the Physical Society of Japan **77**, 034607 (2008).
- ¹⁶ C. Hess, P. Ribeiro, B. Büchner, H. ElHaes, G. Roth, U. Ammerahl, and A. Revcolevschi, Phys. Rev. B **73**, 104407 (2006).
- ¹⁷ K. Kudo, S. Ishikawa, T. Noji, T. Adachi, Y. Koike, K. Maki, S. Tsuji, and K. Kumagai, J. Phys. Soc. Jpn. **70**, 437 (2001).
- ¹⁸ P. Ribeiro, C. Hess, P. Reutler, G. Roth, and B. Büchner, J. Mag. Mag. Mater. **290-291**, 334 (2005).
- ¹⁹ N. Motoyama, H. Eisaki, and S. Uchida, Phys. Rev. Lett. **76**, 3212 (1996).
- ²⁰ M. Matsuda, K. Katsumata, T. Osafune, N. Motoyama, H. Eisaki, S. Uchida, T. Yokoo, S. M. Shapiro, G. Shirane, and J. L. Zarestky, Phys. Rev. B **56**, 14499 (1997).
- ²¹ I. A. Zaliznyak, H. Woo, T. G. Perring, C. L. Broholm, C. D. Frost, and H. Takagi, Phys. Rev. Lett. **93**, 087202 (2004).
- ²² A. Revcolevschi, U. Ammerahl, and G. Dhalenne, Journal of Crystal Growth **198/199**, 593 (1999).
- ²³ C. Hess, B. Büchner, U. Ammerahl, and A. Revcolevschi, Phys. Rev. B **68**, 184517 (2003).
- ²⁴ T. M. Rice, S. Gopalan, and M. Sigrist, Europhys. Lett. **23**, 445 (1993).
- ²⁵ I. A. Zaliznyak, C. Broholm, M. Kibune, M. Nohara, and H. Takagi, Phys. Rev. Lett. **83**, 5370 (1999).
- ²⁶ L. Teske and H. Müller-Buschbaum, Z. Anorg. Allg. Chem. **379**, 234 (1971).
- ²⁷ R. Berman, *Thermal Conduction in Solids* (At the Clarendon Press, Oxford, 1976).
- ²⁸ C. Hess, B. Büchner, U. Ammerahl, L. Colonescu, F. Heidrich-Meisner, W. Brenig, and A. Revcolevschi, Phys. Rev. Lett. **90**, 197002 (2003).
- ²⁹ C. Hess, C. Baumann, and B. Büchner, J. Mag. Mag. Mater. **290-291**, 322 (2005).
- ³⁰ E. Shimshoni, N. Andrei, and A. Rosch, Phys. Rev. B **68**, 104401 (2003).
- ³¹ A. L. Chernyshev and A. V. Rozhkov, Phys. Rev. B **72**, 104423 (2005).
- ³² A. V. Rozhkov and A. L. Chernyshev, Phys. Rev. Lett. **94**, 087201 (2005).
- ³³ For the 4N and 2N compounds we get $l_{0,4N} =$

$(1.56 \pm 0.16) \mu\text{m}$, $T_{u,4N}^* = (204 \pm 11) \text{ K}$, $A_{s,4N} = (58.6 \pm 5.4) \cdot 10^{-16} \text{ m/K}$ and $l_{0,2N} = (305 \pm 5) \text{ nm}$, $T_{u,2N}^* = (217 \pm 3) \text{ K}$, $A_{s,2N} = (78 \pm 1) \cdot 10^{-16} \text{ m/K}$, respectively. Setting $T_{u,2N}^* = T_{u,4N}^* = 204 \text{ K}$ after fitting the 4N data gives $l_{0,2N} = (320 \pm 13) \text{ nm}$ and $A_{s,2N} = (72 \pm 5) \cdot 10^{-16} \text{ m/K}$ for 2N. The errors account for the accuracy of the fit. It is also possible to obtain a good fit with the same A_s for the 4N and 2N cases. However, individual A_s account for errors in the absolute value, while

fixing the energy scale by T_u^* seems physically justified.

³⁴ Modeling l_{mag} with $l_{\text{sp}} \propto \exp(T^*/T)$ which accounts for the alternative scenario of spinons scattering off optical phonons²⁹ results in a fit of similar quality with comparable l_0 and $T^* \sim 300 \text{ K}$.

³⁵ T. Kawamata, N. Kaneko, M. Uesaka, M. Sato, and Y. Koike, unpublished data.